Shape and Size Controlled Deposition of ZnO Thin Films: Comparative Sensitivity towards Methane Gas

N. Mukherjee[1,*], S. Jana[2], H. Chakraborty[3], A. Sinha[3], A. Mondal[2]

[1] *Centre of Excellence for Green Energy and Sensor Systems, Bengal Engineering and Science University, Howrah 711103, West Bengal, India*
[2] *Department of Chemistry, Bengal Engineering and Science University, Howrah 711103, West Bengal, India*
[3] *School of Materials Science and Engineering, Bengal Engineering and Science University, Howrah 711103, West Bengal, India*

The effect of different solutes and solvents on the morphology of Galvanically deposited ZnO thin films is reported here. Hexagonal grains with c – axis orientation were obtained from aqueous $Zn(NO_3)_2$ bath (System A), whereas, the aqueous $ZnSO_4$ bath (System B) yielded cages of ZnO flakes on the xy plane. Almost spherical grains with smaller sizes were obtained from the DMF bath of $Zn(NO_3)_2$ (System C). The highest average roughness (R_a) was shown by the flake like morphology (107.11 nm) and the lowest by the spherical one (16.82 nm). The value of R_a was 21.5 nm for System A. Surface roughness is responsible for adsorbing the test gas, one of the most important factors influencing the sensitivity. Same thing is reflected here by the deposited films for methane sensing. At 300°C, System B showed maximum efficiency (89 %) and the minimum was 69 %, as shown by System C. On the other hand, System A showed an in-between value of efficiency of about 75 %. The response time at 300°C was also lowest for System B, whereas, System A & C showed similar values.

Keywords: Thin Films, Semiconductor, Electrodeposition, Morphology, Methane Sensor.

PACS numbers: 81.15.Pq, 68.55.ag, 61.05.cp, 68.37.Hk, 07.79.Lh, 07.07.Df

1. INTRODUCTION

ZnO is a direct and wide band gap semiconducting material, which is famous for its resourceful applications in the fields of solar cell window material and buffer layer, ultrasonic oscillator, piezo-electronics, transducers, thin film transistors and optoelectronics. The major role of ZnO in the form of thin film is as the sensor for reducing gases [1-4]. Now-a-days, most of the reducing gas sensors are based upon the oxides of Zn and Sn. One advantage of ZnO over other metal oxides is the availability of it in various nano-forms, like wire, belt, spring, sphere, comb, [5-8] etc. Moreover, for ZnO films, the control over the shape and size of the deposited particles can be achieved in a comparatively easy way. As the sensing mechanism is directly related to the amount of gas adsorbed, so, depending on the morphology of the prepared ZnO films, the sensing efficiency may differ. In this work, we report a facile electrochemical route for the shape and size controlled deposition of ZnO thin films on transparent conducting oxide (TCO) coated glass substrates and their comparative sensing capability towards the hazardous gas methane.

2. EXPERIMENTAL DETAILS

2.1 Deposition Procedure

There are many conventional and well described deposition techniques for ZnO thin films, like DC and RF sputtering, metal organic chemical vapor deposition (MOCVD), chemical vapor deposition (CVD), pulsed laser deposition (PLD), electron beam evaporation, spray pyrolysis, sol-gel technique and electrochemical, to name a few [9-15]. Among all these techniques, the electrochemical route has certain advantages, like selective area deposition, minimum wastage of the precursor materials, good control over the reaction kinetics and deposition parameters, and off course, low consumption of energy. Even, for some semiconducting thin films like ZnO and PbX (X = S, Se and Te) a further simplified form [16-20] of the electrochemical technique can be applied, where, the inbuilt cell potential acts as the driving force for the deposition and no external bias is required as the conventional electro-deposition technique. This follows the basic science of a Galvanic Cell and so has been designated as the "Galvanic Technique".

To carry out the deposition of ZnO thin films with three different morphologies, we have prepared three electrolytic baths. The first bath contained 0.01 M aqueous $Zn(NO_3)_2$ solution (System A), the second one was composed of 0.01 M aqueous $ZnSO_4$ solution (System B) and the third bath was prepared by dissolving solid $Zn(NO_3)_2$ in dry dimethylformamide (DMF) to make a 0.01 M solution (System C). Now, a properly cleaned TCO coated glass substrate and a 99.9 % pure metallic Zn rod were dipped in to the working solution to serve as the cathode and the sacrificial anode, respectively for each system. When the two electrodes were short circuited externally, the sacrificial Zn rod dissociates as $Zn \rightarrow Zn^{2+} + 2e$ ($E = + 0.76$ V) and the released electrons reach the TCO cathode by following the external path to carry out the required cathodic reduction for the formation of the films. The optimum temperature for film deposition was found to be 60°C, 30°C and 120°C, respectively for System A, System B

---

* nilsci@yahoo.co.uk

and System C. The depositions were carried out under constant stirring. System A and System C yielded pure ZnO thin films (as deposited), whereas, the as deposited films from System B was found to be composed of a mixed ZnO – Zn(OH)$_2$ phase, which was then converted in to ZnO by post deposition annealing in air at 600°C for 15 minutes. The detailed discussion on the deposition procedure and mechanism has been reported earlier [16, 17] by the authors.

2.2 Characterization Techniques

The deposited films were characterized mainly for their structural and morphological aspects. X-ray diffraction (XRD) patterns were recorded by an X-ray diffractometer (SEIFERT 3000P) using Cu K$_\alpha$ radiation of wavelength $\lambda = 0.15406$ nm. The morphology and surface roughness of the films were studied by atomic force microscopy (AFM) (NT-MDT Solver Pro) in contact mode with a silicon probe having radius of curvature 10 nm, height 15 μm and the standard chip size was 1.6 mm × 1.6 mm × 0.4 mm. The gas-sensing prototype for the films was studied by measuring the change in resistivity between the two contacts made on the ZnO films, before and after passing the test gas methane. The contacts on the films were made by evaporating Pd by e-beam technique. The distance between the two contacts was 1 cm and the area of each contact was 0.3 cm×0.3 cm.

3. RESULTS AND DISCUSSION

3.1 Structural Analysis by XRD

X-ray diffraction measurements of the films were carried out to ascertain the formation of ZnO and also to determine the phase and grain growth. From the XRD patterns (Fig. 1a-d), it can be seen that, pure ZnO films were directly obtained from System A and System C (Figs. 1a & 1d, respectively). On the other hand, System B yielded a mixed ZnO – Zn(OH)$_2$ phase film (Fig. 1b), which then converted in to pure ZnO by annealing in air at 600°C for 15 minutes (Fig. 1c). For all the cases, polycrystalline grain growth was observed. Scherrer equation (*grain size (D) = 0.9λ/(βcosθ) [where λ is the wave length of the X-radiation (here 1.54056 Å), β is the value of full-width at half-maxima (FWHM) of the most intense peak and θ is the half of the diffraction angle of the corresponding peak]*) has been applied to calculate the crystallite sizes of the films grown from System A and C, as the equation can only be applied for the crystals with regular shapes like spherical, hexagonal or cubic. The average crystallite sizes of the films calculated to be about 500 nm, for System A, and 100 nm for System C. The results have been matched with the JCPDS card No. 05-0664 for ZnO. The '*' marked peaks in the XRD patterns correspond to the lower lying SnO$_2$ of the TCO glass.
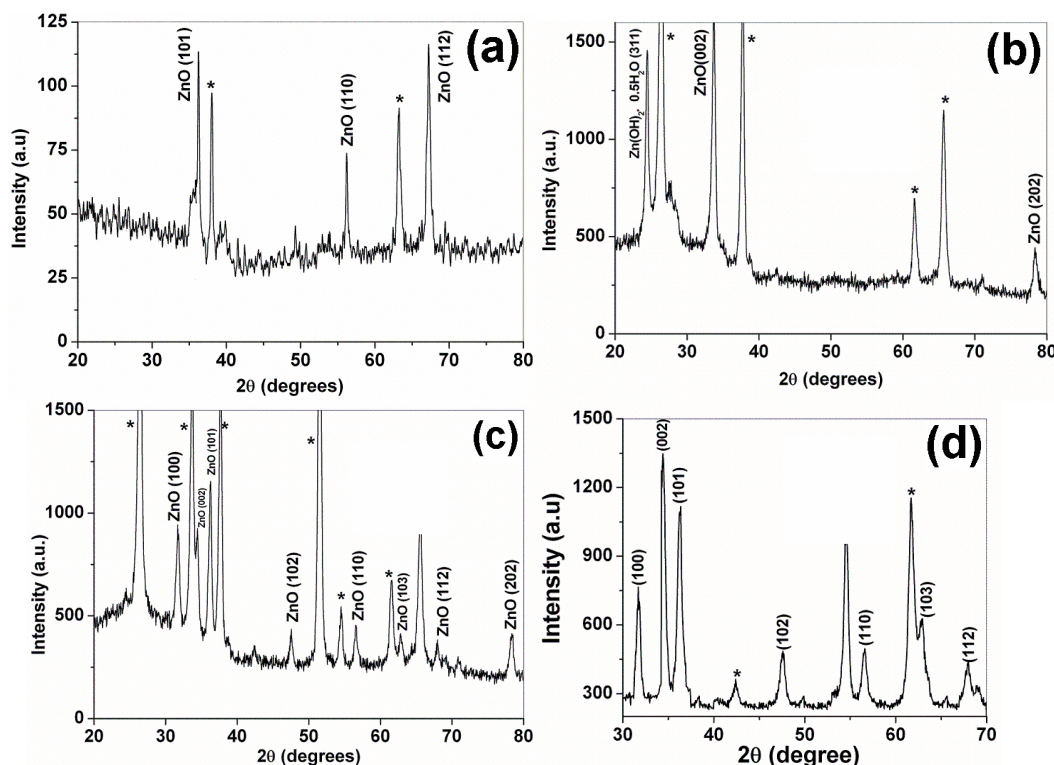

Fig. 1 – XRD patterns of the films deposited from (a) System A (b) System B (c) System B after annealing and (d) System C

3.2 Morphological Analysis by AFM

The AFM image for System A (Fig. 2a) revealed hexagonal columnar growth along c – axis, whereas, System B showed (Fig. 2b and after annealing, Fig. 2c) cages of ZnO flakes, grown on 'xy' plane. Fig. 2d is the representative AFM image of the films obtained from System C, from which, the formation of almost spherical ZnO grains are evident. The average grain diameters as obtained from the AFM images were 400 nm, 2.0 μm and 100 nm, respectively for System A, B & C. These values are in good

agreement with what we have obtained from the XRD measurements. No significant change in morphology was obtained after annealing for the films obtained from System B. So, it can be inferred that this 'Galvanic' route is highly effective for the shape and size controlled deposition of ZnO thin films. The highest average roughness (R_a) was shown by the flake like morphology (107.11 nm) i.e. System B after annealing, and the lowest by the spherical one (16.82 nm). The value of R_a was 21.53 nm for Sys-

tem A. It is a well-known fact that, adsorption of gases increases with increasing porosity and surface roughness, and hence, there is a good chance of using these ZnO films as gas sensors. It is expected that the annealed films of System B with highest R_a value, could serve as a good gas sensor among the three, which is discussed in detail in the next section.
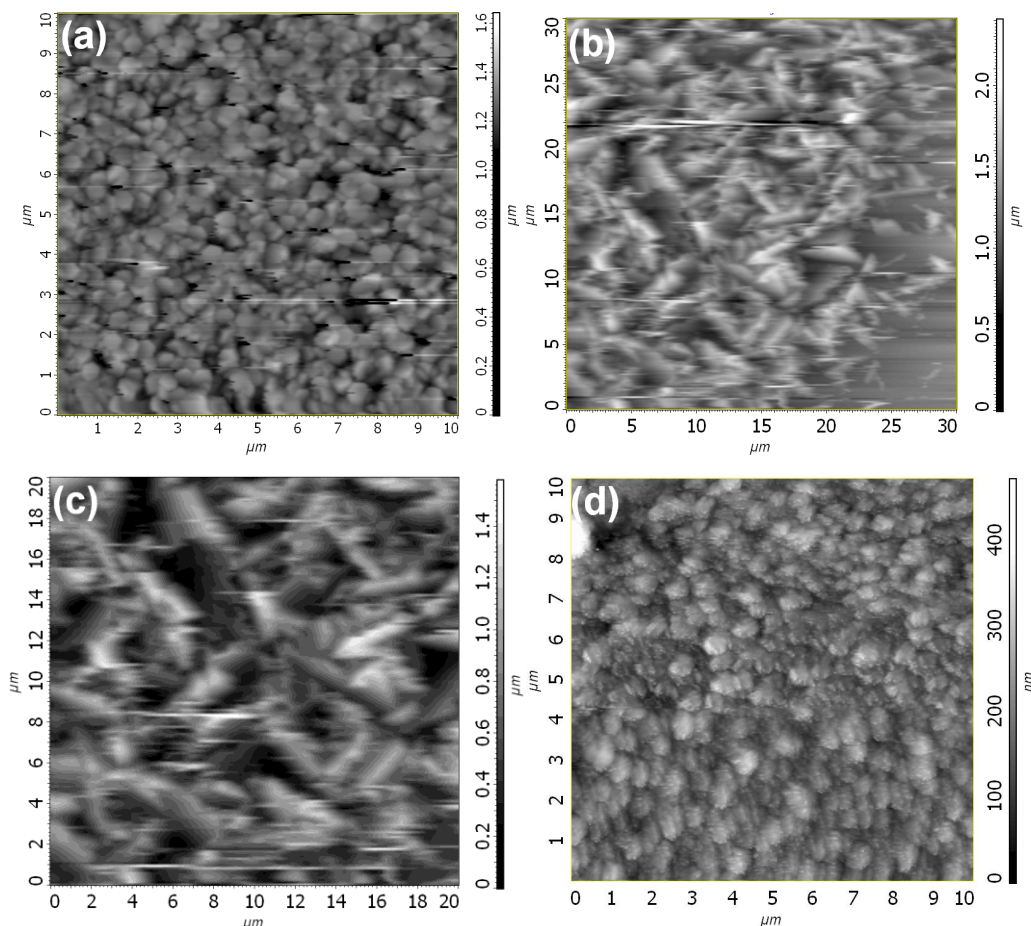

Fig. 2 – AFM images of the films deposited from (a) System A (b) System B (c) System B after annealing and (d) System C

3.3 Methane Sensor Prototype

The sensor studies were carried out inside a closed glass tube ($\varnothing = 10$ cm $\times$ 4 cm) with inlet and outlet for gases and it was placed coaxially inside a resistively heated furnace with 4 cm constant temperature zone. The temperature was controlled within $\pm 1°C$ using copper constantan thermocouple in-built in a precise temperature controller. Electrical connections were taken by using fine copper wire and silver paste for the metallization contacts. High purity (100 %) methane gas and IOLAR grade N_2 (carrier gas) in desired proportions were allowed to flow to the gas-sensing chamber through a mixing path via mass flow controller & the mass flow meter, respectively. The mass flow rate and thus the relative concentrations of the gases were kept constant throughout the experiment. The gas pressure over the sensor device was 1 atmosphere during the experiment. The current–voltage and resistivity characteristics of the sensors in

presence and absence of methane was measured by a Kithley 6487 voltage source picoammeter; applying a constant voltage of 2.0 V. The percentage sensitivity to 1 % CH_4 concentration was recorded at different operating temperatures to find out the optimum temperature for highest sensitivity. The percentage sensitivity (S) is expressed as:

$$S = (R_g - R_{air})/R_{air} \times 100 \%$$

Where, R_g and R_{air} are the resistivities of the film in presence of CH_4 gas and dry air, respectively. The results obtained for different films are summarized in Table 1. Maximum efficiency of about 89 % was observed for the annealed film obtained from System B which in shown Fig. 3a. For all cases, maximum sensing efficiency was observed at 300°C, which was found to be the optimum temperature of operation for this sensing devices. This indicates that, a steady equilibrium between adsorption and desorption of CH_4

had been established at this temperature. Increasing the temperature above 300°C, the rate of desorption of CH_4 predominates over the rate of adsorption, which in turn, brings down the gas-sensing efficiency. It is evident from Table 1 that, as the surface roughness of the ZnO film increases, there is a significant increase in the efficiency and decrease in the response time

(Fig. 3b). As the films obtained from System A and System C have no notable difference in their R_a values, their response times and efficiencies are also close. The highly porous nature of the deposited films from System B helps in better adsorption of the test gas, which also helps in increasing its efficiency.
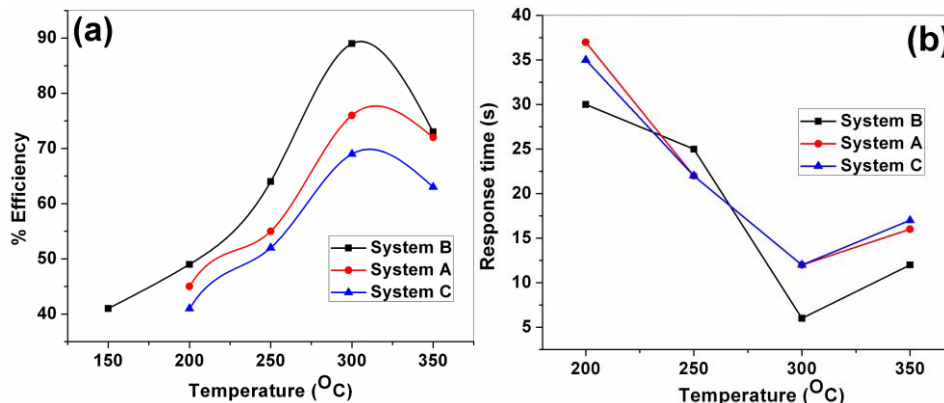

Fig. 3 – (a) plot for % efficiency vs. temperature and (b) response time vs. temperature for the methane sensor prototype fabricated using ZnO thin films with three different morphologies

Table 1 – Appointment of special paragraph styles

№	System	Morphology	Average grain diameter	Surface roughness (nm)	Response time (s)	Recovery time (s)	Efficiency (%)
1	System A	Hexagonal rod	400 nm	21.53	12	25	74.75
2	System B (annealed)	Flakes and cages	2.0 μm	107.11	06	20	89.10
3	System C	Spherical	100 nm	16.82	12	35	69.10

4. CONCLUSION

A facile route for synthesizing shape and size controlled ZnO thin films on transparent conducting oxide coated glass substrates has been reported. A comparative study on the various structural properties of the deposited films and their morphology dependent methane sensing capabilities have been carried out. It has been established that, films with high surface roughness and porosity can serve as a better methane

sensor prototype. The activation temperature was also found to be low for such sensors.

REFERENCES

1. Y. Nakamura, H. Yoshioka, M. Miyayama, H. Yanagida, *J. Electrochem. Soc.* **137**, 940 (1990).
2. J.D. Choi, G.M. Choi, *Sens. Actuators B* **69**, 120 (2000).
3. J.H. Yu, G.M. Choi, *Sens. Actuators B* **75**, 56 (2001).
4. H. Nanto, H. Sokooshi, T. Kawai, *Sens. Actuators B* **14**, 715 (1993).
5. Z.L. Wang, *Mater. Today* **7**, 26 (2004).
6. D.P. Norton, Y.W. Heo, M.P. Ivill, K. Ip. S.J. Pearton, M.F. Chisholm, T. Steiner, *Mater. Today* **7**, 34 (2004).
7. X. Wang, Q. Li, Z. Liu, J. Zhang, Z. Liu, R. Wan, *Appl. Phys. Lett.* **84**, 4941 (2004).
8. Z.L. Wang, *J. Phys.: Condens. Matter* **16**, R829 (2004).
9. J.H. Yu, G.M. Choi, *Sens. Actuators B* **75**, 56 (2001).
10. S. Bethke, H. Pan, B.W. Wessels, *Appl. Phys. Lett.* **52**, 138 (1988).
11. B. Sang, M. Konagai, *Jpn. J. Appl. Phys.* **35**, L602 (1996).
12. A. Kuroyanagi, *Jap. J. Appl. Phys.* **28**, 219 (1989).
13. J.De. Merchant, M. Cocivera, *Chem. Mater.* **7**, 1742 (1995).
14. T. Pauporté, D. Lincot, *Electrochim. Acta* **45**, 3345 (2000).
15. S. Sakohara, L.D. Tickanen, M.A. Anderson, *J. Phys. Chem.* **96**, 11086 (1992).
16. A. Mondal, N. Mukherjee, S.K. Bhar, *Mater. Lett.* **60**, 1748 (2006).
17. N. Mukherjee, Sk.F. Ahmed, K.K. Chattopadhyay, A. Mondal, *Electrochim. Acta* **54**, 4015 (2009).
18. A. Mondal, N. Mukherjee, *Mater. Lett.* **60**, 2672 (2006).
19. A. Mondal, N. Mukherjee, S.K. Bhar, D. Banerjee, *Thin Solid Films* **515**, 1255 (2006).
20. N. Mukherjee, Sk.F. Ahmed, D. Mukherjee, K.K. Chattopadhyay, A. Mondal, *phys. status solidi C* **5**, 3458 (2008)